

## High-pressure specific-heat spectroscopy at the glass transition in *o*-terphenyl

H. Leyser,<sup>1,2</sup> A. Schulte,<sup>1</sup> W. Doster,<sup>2</sup> and W. Petry<sup>2</sup>

<sup>1</sup>*Department of Physics, University of Central Florida, Orlando, Florida 32816-2385*

<sup>2</sup>*Physik Department E13, Technische Universität München, D-85748 Garching, Federal Republic of Germany*

(Received 23 November 1994)

Measurements of the enthalpy relaxations in liquid orthoterphenyl in the supercooled state have been carried out using specific-heat spectroscopy over the frequency range from 2 Hz to 6.3 kHz, as a function of temperature and as a function of pressure. The observed  $\alpha$ -relaxation peaks in the phase of the complex specific heat show increasing relaxation times  $\tau$  with increasing pressure at constant temperature, similar to the divergence of  $\tau$  when the calorimetric glass temperature  $T_g$  is approached by lowering the temperature at constant pressure. The temperature and pressure dependence of the measured mean relaxation times  $\bar{\tau}$  near  $T_g$  are in remarkable agreement with those found by other spectroscopic methods and have been compared with an extended Vogel-Fulcher-Tammann law. However, we find different scaling when the glass transition is approached by cooling or by increasing pressure. This suggests that the assumption of a simple volume-activated process is not adequate.

PACS number(s): 64.70.Pf, 65.20.+w, 07.35.+k, 61.25.Em

### INTRODUCTION

The glass transition is a universal phenomenon occurring in systems with a wide range of molecular weights and chemical bonding [1]. Examples include van der Waals liquids, computer modeled hard spheres, polymers, and biomolecules. In the transition region the dynamics is determined by a dramatic slowing down of structural ( $\alpha$ -) relaxations [2], which have been investigated extensively as a function of temperature. Though in isothermal viscosity measurements a similar divergence of the mean relaxation time as a function of pressure has been observed [3], experiments yielding information on the relaxation spectrum, most importantly with a probe which couples to all degrees of freedom, are scarce. This poses the question of whether there are differences in the dynamics if the glass transition is approached by temperature changes or isothermal density changes.

Molecular dynamics computations [4] and high-pressure studies of the static diffusivity in liquid methylcyclohexane [5] have shown that structural arrest, a signature of the glassy state, occurs above a critical density. In this region, the diffusion coefficient follows a Doolittle equation  $D = D_0 \exp[-A/(V - V_0)]$ . A theoretical justification is based on the free volume model introduced by Cohen and Turnbull [6] and substantiated by Cohen and Grest [7]. Assuming a linear relation between volume and temperature leads to the Vogel-Fulcher-Tammann (VFT) law, which is often used to parametrize in the viscous region the temperature dependence of the  $\alpha$  relaxation over a wide range. To higher temperatures, i.e., towards the liquid state, the relaxation becomes more Arrhenius-like. When the mean relaxation time of a viscous liquid exceeds the experimental time scale, the system falls out of equilibrium, thus defining the calorimetric glass transition temperature  $T_g(\tau)$ .

An alternative approach to supercooled liquid dynamics has been provided by the mode coupling theory (MCT) [2]. Here a transition on a mesoscopic time scale from an ergodic (liquid) to a nonergodic (arrested) state has been postulated at a temperature  $T_c$  typically several tens of degrees above  $T_g$ . Density relaxations around  $T_c$  are predicted to follow scaling laws and indicating a transition in the main relaxation mechanism from a localized, cagelike motion below  $T_c$  to long range structural relaxations identified with the  $\alpha$  process above  $T_c$ . In the idealized MCT the mean  $\alpha$ -relaxation time is supposed to follow a power law diverging at  $T_c$  with an exponent related to the scaling laws of the density correlation. Ergodicity restoring processes or  $\alpha$  relaxation below  $T_c$  have been taken into account in an extended version [8,9]. Depending on the system, both Arrhenius and VFT laws are possible for the mean relaxation time at temperatures below  $T_c$  [9]. For nonassociated or fragile glass formers direct observation of the density fluctuations by neutron [10–12] and light scattering [13,14] experiments indicate qualitative to quantitative agreement with the MCT. In particular, the predicted power law for the mean relaxation time fits experimental data above  $T_c$  well [2,15,16].

Indications for a change in the relaxation mechanism around  $T_c$  have also been found by nonspectroscopic methods. Jump rates in orthoterphenyl (OTP) deduced from tracer diffusion and alternatively from viscosity diverge around  $T_c$  [17]. For a large number of nonassociated glass formers renormalized relaxation rates show a bending over in a temperature range typically some tens of a degree above  $T_g$  [18,19].

Here we use temperature *and* pressure as independent variables to approach the glass transition on different trajectories in phase space. By using pressure as an additional variable the effects of volume and temperature on molecular motions can be separated. If the glass transi-

tion is a simple volume-activated process, there should be a universal temperature-pressure superposition principle for any fixed relaxation time.

Specific-heat spectroscopy measures contribution from all degrees of freedom of the system, contrary to many other methods of relaxation spectroscopy. In addition, specific-heat spectroscopy has advantages in nonpolar substances such as OTP, where dielectric spectroscopy is difficult to perform. On the other hand, specific-heat spectroscopy is limited to a frequency range from 0.1 Hz to 10 kHz, i.e., relaxations can only be measured close to  $T_g$ . In particular, mesoscopic time scales cannot be reached and no direct comparison to MCT can be expected.

OTP is one of the best studied glass forming substances. Although it strongly tends to crystallize, it is widely used for studies on the glass transition because the temperature range of the supercooled state is around room temperature. Further, structural arrest can be reached under moderate pressure. It is a prototype of a nonassociated or fragile glass former, i.e., the temperature variation of the viscosity deviates strongly from a simple Arrhenius law. OTP melts at  $T_m = 339$  K and for atmospheric pressure a calorimetric glass transition temperature  $T_g = 243$  K is found. At this temperature, the viscosity has a value of roughly  $10^{13}$  P, which corresponds to a mean relaxation time of about  $10^3$  s. The mode coupling cross over temperature  $T_c$ , where localized motions desintegrate to long range structural relaxations, has been established to be at  $\sim 290$  K [12,14,15].

Dixon and Nagel [20] have measured the frequency dependent specific heat  $c_p(\omega)$  and thermal conductivity  $\kappa$  of OTP-phenylphenol mixtures under atmospheric pressure. These experiments have shown that all the dynamics is contained in  $c_p(\omega)$  and that  $\kappa$  is frequency independent.

In the following we focus on pure OTP, which is a simple monomolecular system. Having overcome the problems of crystallization, we present the first measurements of the dynamic specific heat at variable pressure and temperature.

## EXPERIMENTAL SECTION

Specific-heat spectroscopy has been performed using the technique of Birge and Nagel [21]. A thin plane rectangular Ni-film heater on a glass substrate immersed in the sample liquid also acts as the thermometer. Exponentially damped heat waves dissipate into the substrate and into the viscous sample along a static temperature gradient. The temperature oscillation at the Ni film has the same frequency  $2\omega$  as the heat oscillation and lags in phase by  $\frac{\pi}{4}$ . The amplitude of this temperature oscillation depends on the thermal effusivities  $\epsilon(\omega)$  of the sample and the substrate, which are the product of specific heat  $c_p(\omega)$ , thermal conductivity  $\kappa$ , and mass density  $\rho$  for the surrounding media. In the glass transition region, the mean enthalpy relaxation times are on the same time scale as the inverse measuring frequencies, leading to a frequency-dependent specific heat. In this dispersion region, an additional phase shift of the complex specific

heat is obtained as requested by the Kramers-Kronig relation. The complex frequency-dependent specific heat  $c_p(\omega) = c_p'(\omega) + ic_p''(\omega)$  of the sample can be calculated from the measured voltage drop of the resistance thermometer after a calibration run of the empty cell.

Our specific-heat spectrometer has been described in detail elsewhere [22]. The improved version uses voltage controlled current sources instead of ordinary resistors in the bridge [23]. The resistance of the Ni film, which yields the average temperature, was measured precisely by balancing the bridge with a remote controlled adjustable reference resistor and using the four-wire technique. Due to the signal to noise ratio, the upper frequency limit for the heat oscillations in our setup was 6.3 kHz. The lower limit reached 2 Hz, as given by the lock-in amplifier. The glass substrate (25.4 mm, 4 mm thick) with a Ni film supporting the sample was placed in a cylindrical high-pressure cell. A copper-beryllium disk holding the glass substrate and matching the core provided thermal coupling to the CuBe cell. A gas pressure system (Newport Scientific), working with nitrogen gas, provided hydrostatic conditions and a maximum pressure of 206.8 MPa (30000 psi). Electrical feedthroughs into the high pressure were made by sealing the copper wires into a pipe with epoxy resin. The high-pressure cell was temperature controlled with a LakeShore DRC 93 controller using a Pt100 platinum resistor as sensor.

Orthoterphenyl was obtained from Aldrich (> 99%) and used without further purification. The OTP was molten and filled into the carefully cleaned high-pressure cell until it covered the Ni film of the specific-heat experiment. After sealing the cell, it was heated to 340 K for 30 min to ensure that the OTP had melted. Dipping the high-pressure cell into liquid nitrogen cooled the sample down to 240 K in 1 min, thus avoiding crystallization. Below 275 K the supercooled state was stable far beyond the measuring times. At 285 K crystallization occurred in a few minutes which resulted in an abrupt change of the signal. Data from crystallized samples were rejected.

Dynamic specific-heat measurements were performed at atmospheric pressure as a function of temperature (0.1 MPa, 245–280 K) and at two fixed temperatures as a function of pressure (268 K, 0.1 MPa–82.7 MPa in steps of 6.9 MPa and 275 K, 0.1 MPa–103.4 MPa in steps of 6.9 MPa). A pressure of 104 MPa was sufficient to observe a drop in the dispersive part of  $c_p$  corresponding to the calorimetric glass temperature  $T_g(\omega)$ . More than three decades in frequency (2 Hz, 6.3 Hz, 20 Hz–6.3 kHz) were covered. After each run it was verified that the sample had not crystallized.

With a plane film geometry one measures the thermal effusivity  $\epsilon$ , which is the product of the specific heat  $c_p$ , the thermal conductivity  $\kappa$ , and the mass density  $\rho$  of the sample. However,  $\kappa$  and  $\rho$  do not show a significant dependence on frequency [20] so that the frequency dependence of the specific heat  $c_p(\omega)$  is well represented by the frequency dependence of the thermal effusivity  $\epsilon(\omega)$ . The contribution of the glass substrate to the thermal effusivity  $\epsilon(\omega)$  was measured for the same frequencies, temperatures, and pressure without the sample in the cell and subtracted.

## RESULTS AND DISCUSSION

Figure 1 shows the amplitude  $|\epsilon(\omega)|$  and phase  $\varphi(\omega)$  of the complex thermal effusivity  $\epsilon(\omega) = |\epsilon(\omega)|e^{i\varphi(\omega)}$  as a function of temperature ( $P = 0.1$  MPa) for selected frequencies in the dispersion region. The temperature where the amplitude of  $\epsilon(\omega)$  drops is strongly depending on frequency, and indicates the characteristic relaxation time in the viscous liquid as  $T$  is lowered. At the same temperature there is a peak in the phase in agreement with the Kramers-Kronig relation. The data for all frequencies were fitted to a Cole-Davidson function

$$\epsilon(\omega) = (1 - \delta\epsilon) + \delta\epsilon(1 + i\omega\tau_0^{CD})^{-\beta_{CD}} \quad (1)$$

(shown as dashed lines in Figs. 1 and 2) resulting in a distribution parameter of  $\beta_{CD} = 0.55 \pm 0.05$ . (The range we found for the Cole-Davidson exponent  $\beta_{CD}$  is in accordance [24] with the value of the von Schweidler exponent  $b = 0.55-0.65$  found in neutron and light scattering studies [15,14].) The error bars of our measurements are too large to speculate about any temperature dependence of  $\beta_{CD}$ .

In Fig. 2 we present amplitude and phase of the complex thermal effusivity in the dispersion region as a function of pressure ( $T = 268$  K) for selected frequencies. The features which correspond in Fig. 1 to a decrease in temperature are now observed with increasing pressure. In particular, the drop in the dispersive part of  $\epsilon(\omega)$  exhibits a strong frequency dependence and has the same magnitude. It indicates an increase of the characteristic relaxation time in the liquid as the pressure is raised. Fitting the relaxation process to the Cole-Davidson function (1) (dashed lines in Fig. 2), we find the same  $\beta_{CD} = 0.55 \pm 0.05$  as for the variable temperature data in Fig. 1. Within experimental accuracy, our data demonstrate that the dynamic specific heat near the glass transition exhibits the same features, whether the liquid is cooled towards  $T_g$  or pressurized toward a glass transition pressure  $P_g$ .

The calorimetric glass temperature or pressure for each frequency was determined from the midpoint of the step of the amplitude in the thermal effusivity. The mean relaxation times  $\bar{\tau}$  are then calculated from the frequencies  $f$  using

$$\frac{1}{\bar{\tau}} = 2\pi fc, \quad (2)$$

where  $c$  is a small correction factor ( $c \approx 0.77$ ) to obtain the mean relaxation times from the frequencies with respect to the distribution of relaxation times in the system. This is necessary since the mean relaxation time is not found at the inverse of the frequency  $f$  where the amplitude drops to half of the stepsize. For the Cole-Davidson function the mean relaxation time  $\bar{\tau}$  is given by  $\bar{\tau} = \tau_0^{CD}\beta_{CD}$  [25], whereas the half step of the amplitude for  $\delta\epsilon = 0.3$  and  $\beta_{CD} = 0.55$  is found at  $0.42\tau_0^{CD}$ .

The mean relaxation time is displayed in Fig. 3 as a function of the inverse temperature at  $P = 0.1$  MPa. The data from specific-heat spectroscopy prove to be compatible to data from dielectric spectroscopy (DS) [26] and

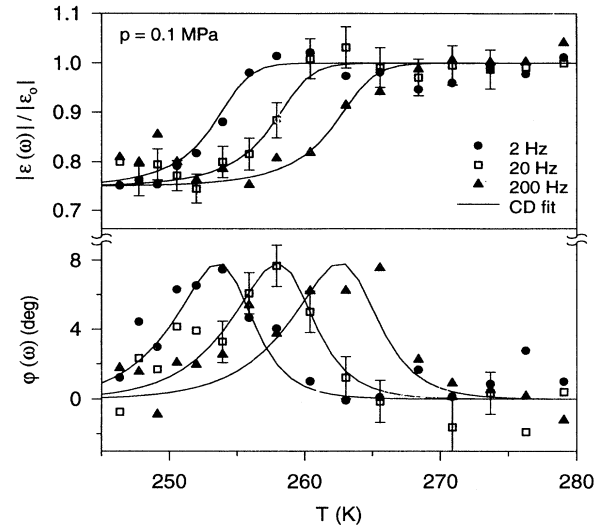


FIG. 1. Amplitude and phase of the thermal effusivity  $\epsilon(\omega)$  in orthoterphenyl as a function of temperature at atmospheric pressure. The amplitude is normalized to the low frequency limit  $\epsilon_0$  of the thermal effusivity. Data are shown for three measurement frequencies. The relaxation times have been determined from the amplitude only. The size of the error bars is typical for all frequencies.

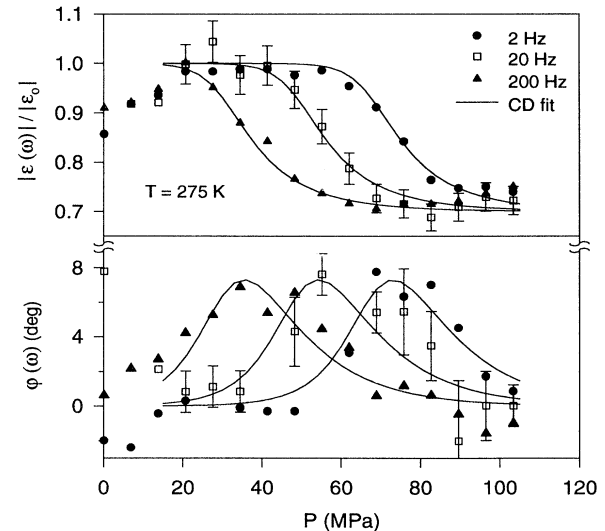


FIG. 2. Amplitude and phase of the thermal effusivity  $\epsilon(\omega)$  in orthoterphenyl as a function of pressure at  $T = 275$  K. The amplitude is normalized to the low frequency limit  $\epsilon_0$  of the thermal effusivity. Data are shown for three measurement frequencies. The relaxation times have been determined from the amplitude only. The size of the error bars is typical for all frequencies. Below 20 MPa, data could not be taken in complete equilibrium due to fast pressurizing in that range.

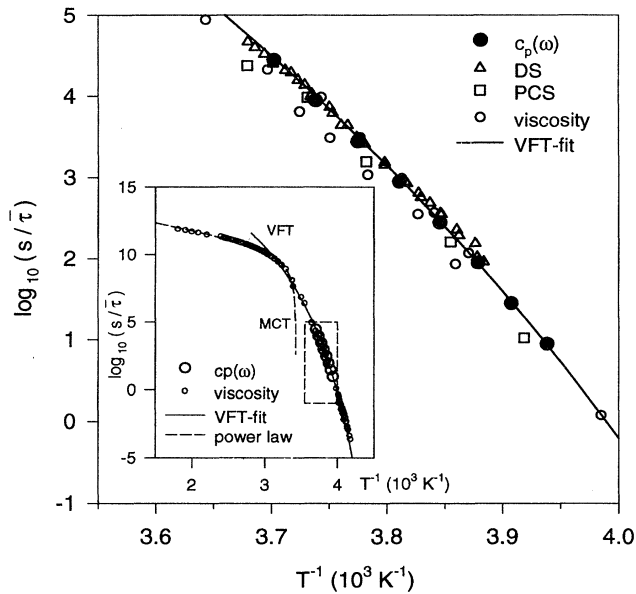


FIG. 3. Activation plot of the mean relaxation times  $\bar{\tau}$  of orthoterphenyl at  $p = 0.1$  MPa. Error bars are represented by the symbol size. Specific-heat data are compared with PCS, DS, and viscosity data. Below 326 K, the viscosity follows the Vogel-Fulcher-Tammann law (solid line). Above 290 K, the viscosity data are well represented by a power law (dashed line) from the MCT.

photon correlation studies (PCS) [27] and to viscosity data [28]. Parametrizing the data in the viscous range with the VFT law

$$\bar{\tau} = \overline{\tau_{VFT}} e^{B/(T-T_0)}, \quad (3)$$

we obtain  $\log_{10}(\overline{\tau_{VFT}}/s) = -18.2 \pm 0.15$ ,  $B = (2500 \pm 50)$  K and  $T_0 = (191 \pm 2)$  K fitting our measurements and additional viscosity data from [28]. According to previous data analysis [29], an upper limit at 326 K for the applicability of the VFT equation has been assumed. (Above a crossover region of 290–326 K power laws as proposed by the MCT represent the measured mean relaxation times very well. An Arrhenius law as proposed in [29,14] poorly describes the data.)

In Fig. 4 the mean relaxation times are plotted versus pressure for the temperatures  $T = 268$  K and  $T = 275$  K and compared to relaxation times measured with DS and PCS. In the limited experimental pressure range, the PCS and DS data have been interpolated to  $T = 268$  K and  $T = 275$  K and the DS data have been corrected to the mean relaxation times with respect to the distribution of the relaxation times for the same reasons as in Fig. 3 before. Again fair agreement is found between the different spectroscopic measurements. The pressure dependence can be described very well with an activation form

$$\bar{\tau} = \bar{\tau}_A e^{PV^*/RT}. \quad (4)$$

We find the activation volumes  $V^* = (310 \pm 10)$  cm<sup>3</sup>/mol

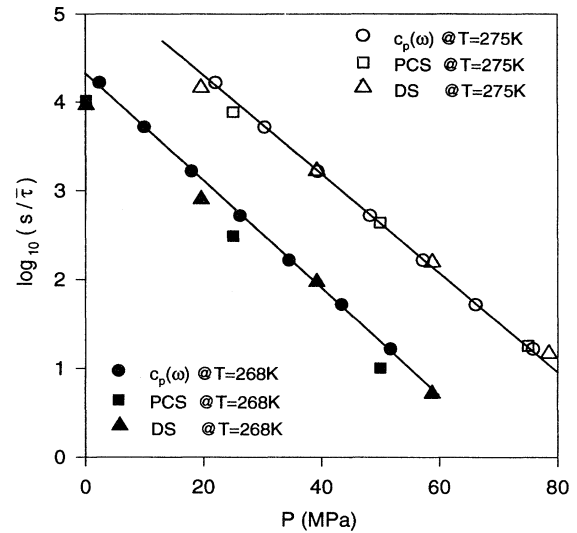


FIG. 4. Mean relaxation times  $\bar{\tau}$  of orthoterphenyl versus pressure at two fixed temperatures,  $T = 268$  K and  $T = 275$  K. Error bars are represented by the symbol size. Specific heat data are compared with PCS and DS data.

for  $T = 268$  K and  $(293 \pm 10)$  cm<sup>3</sup>/mol for  $T = 275$  K, which is  $514 \text{ \AA}^3$  and  $487 \text{ \AA}^3$  per molecule, respectively. This can be compared with the specific volume and the molecular volume of liquid OTP, which is  $219 \text{ cm}^3/\text{mol}$  or  $363 \text{ \AA}^3$  per molecule [30]. Because the latter volume is smaller than the activation volume, cooperative effects must be important.

The data in Figs. 3 and 4 allow us to investigate whether the specific volume is the essential variable determining the mean relaxation time  $\bar{\tau}$ . The specific volumes  $V(T, P)$  for the temperatures and pressure of our experiments were determined from pressure-volume-temperature relations of OTP measured by Naoki and Koeda [31] and parametrized by a polynomial in  $T$  and  $P$ . Figure 5 shows the mean relaxation time  $\bar{\tau}$  versus the inverse specific volume  $V^{-1}(T, P)$ , proving that temperature or pressure variation when scaled on the same specific volume do not give identical results.

Pressure changes the density, whereas varying the temperature alters the volume as well as the thermal energy. However, the mean relaxation time at *constant pressure* and variable temperature is well characterized by the Doolittle equation

$$\ln(\bar{\tau}/\bar{\tau}_D) = \frac{A}{V(T) - V_0}. \quad (5)$$

A least squares fit to the data yields  $\log_{10}(\bar{\tau}_D/s) = -18.05 \pm 0.15$ ,  $A = (357 \pm 3)$  cm<sup>-3</sup> mol<sup>-1</sup>, and  $V_0 = (197.8 \pm 0.1)$  cm<sup>-3</sup> mol<sup>-1</sup>. Because the pressure dependence of  $\bar{\tau}$  is well represented by Eq. (4),  $\log_{10}(\bar{\tau})$  data derived from pressure variation show no curvature over the range of our measurements.

To unify temperature and pressure dependence, one could consider a generalized form of the VFT equation

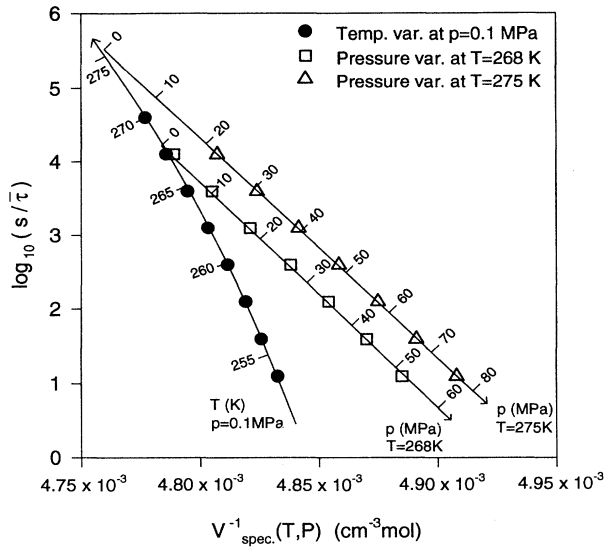


FIG. 5. Mean relaxation times  $\bar{\tau}$  of orthoterphenyl as a function of the inverse specific volume. Error bars are represented by the symbol size.

(3) as proposed by Cohen and Grest [7] with

$$\begin{aligned} T_0 &\rightarrow T_0 + aP, \\ B &\rightarrow B + bP. \end{aligned} \quad (6)$$

Keeping  $B = 2500$  K and  $T_0 = 191$  K fixed from the application of Eq. (3) to the 0.1 MPa pressure data and fitting all pressure data to the generalized VFT Eqs. (3) and (6), all data can be plotted onto one master curve (Fig. 6),

$$\ln(\bar{\tau}/\bar{\tau}_0) = \frac{B + b(P - 0.1 \text{ MPa})}{T - [T_0 + a(P - 0.1 \text{ MPa})]} \equiv X, \quad (7)$$

where  $a = 0.3$  K/MPa and  $b = 0.29$  K/MPa. The parameters we find to fit the data neither coincide to those found by Fytas *et al.* [27] in photon correlation studies [ $\bar{\tau}_0 = 1.5 \pm 0.8 \times 10^{-12}$  s,  $B = (921 \pm 17)$  K,  $T_0 = 219$  K,  $a = (0.56 \pm 0.03)$  K/MPa, and  $b = 0.2$  K/MPa] nor to those found by Naoki *et al.* [26] by means of dielectric measurements ( $\bar{\tau}_0 = 8.9 \times 10^{-22}$  s,  $B = 3779$  K,  $T_0 = 170$  K,  $a = 3.43$  K/MPa, and  $b = 0.19$  K/MPa). Because they use only the limited frequency range of their measurements for fitting with Eq. (7), their fit parameters do not match to the extended viscosity data in Fig. 3 at atmospheric pressure. Relying only on the limited frequency range of their PCS and dielectric measurements, a manifold of  $B - T_0$  combinations fit the data locally. Fixing  $B$  and  $T_0$  from the 0.1 MPa data, it is impossible to scale all data onto line  $\ln(s/\tau) = -X$  with slope  $-1$  with the additional  $aP$  and  $bP$  terms in the extended VFT formula. The data from isothermal measurements deviate significantly from the master line at slow relaxation times or high viscosities.

Thus a universal pressure-temperature superposition principle cannot be found for the fragile glass former OTP in terms of the free volume model and the gen-

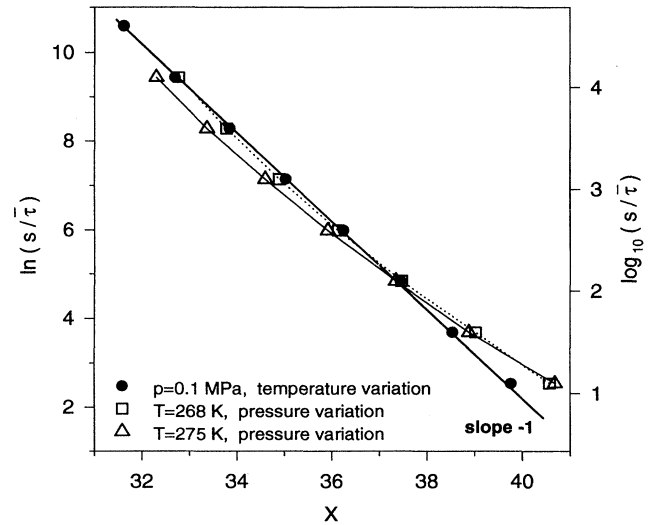


FIG. 6. Mean relaxation times  $\bar{\tau}$  of orthoterphenyl plotted against the exponent  $X$  of the extended Vogel-Fulcher-Tammann law. Error bars are represented by the symbol size. All data should match a master line with slope  $-1$ .

eralized Vogel-Fulcher-Tammann Eq. (7). To check the validity of Eq. (5) or (7), it is not sufficient to vary only temperature or pressure, as it was done for the viscosity under pressure for several simple liquids [3] in a wide range at a given fixed temperature. At least the glass transition in OTP cannot be characterized by a simple volume-activated process.

## CONCLUSION

We have studied the temperature and pressure-dependent dynamic specific heat of supercooled orthoterphenyl near the glass transition using specific-heat spectroscopy. The mean enthalpy relaxation times from one isobaric measurement at atmospheric pressure and two isothermal measurements at  $T = 268$  K and  $T = 275$  K are compared with an extended Vogel-Fulcher-Tammann law, varying  $B$  and  $T_0$  linear in pressure. The poor applicability of this equation for the fragile glass former OTP contradicts the assumption of a simple volume-activated process in the picture of the free volume model. Our measurements point to the importance of high-pressure studies of the dynamics in the supercooled liquid to disentangle thermal and volume effects.

A direct comparison of our data with the predictions of the mode coupling theory is not possible because specific-heat spectroscopy measures in the long time limit, which is beyond the mesoscopic time range where the scaling laws are predicted. Inelastic neutron and light scattering experiments under pressure which measure the dynamical response in the mesoscopic time range are in preparation. However, the measurements presented here indicate that the dynamical response along the various trajectories through phase space (pressure and temperature variation) will be different.

## ACKNOWLEDGMENTS

We wish to thank Professor W. Götze for helpful discussions and Dr. L. Chow for his patience while evaporating the Ni films. This work was partly supported by the National Science Foundation (Grant No. MCB-9305711) and the Deutsche Forschungsgemeinschaft (Do. 241/2-1).

orating the Ni films. This work was partly supported by the National Science Foundation (Grant No. MCB-9305711) and the Deutsche Forschungsgemeinschaft (Do. 241/2-1).

- 
- [1] J. Wong and C. A. Angell, *Glass Structure by Spectroscopy* (Dekker, New York, 1976).
- [2] W. Götze and L. Sjögren, *Rep. Prog. Phys.* **55**, 241 (1992).
- [3] C. A. Herbst, R. L. Cook, and H. E. King Jr., *J. Non-Cryst. Solids* **172**, 265 (1994).
- [4] L. V. Woodcock and C. A. Angell, *Phys. Rev. Lett.* **47**, 1129 (1981).
- [5] J. Jonas, D. Hasha, and S. G. Huang, *J. Chem. Phys.* **71**, 3996 (1979).
- [6] M. H. Cohen and D. Turnbull, *J. Chem. Phys.* **31**, 1164 (1959).
- [7] M. H. Cohen and G. S. Grest, *Phys. Rev. B* **20**, 1077 (1979).
- [8] W. Götze and J. Sjögren, *Z. Phys. B* **65**, 415 (1987); *J. Phys. C* **21**, 3407 (1988).
- [9] L. Sjögren, *Z. Phys. B* **79**, 5 (1990).
- [10] W. Knaak, F. Mezei, and B. Farago, *Europhys. Lett.* **7**, 529 (1988).
- [11] B. Frick, R. Zorn, D. Richter, and B. Farago, *J. Non-Cryst. Solids* **131**, 169 (1991).
- [12] J. Wuttke, M. Kiebel, E. Bartsch, F. Fujara, W. Petry, and H. Sillescu, *Z. Phys. B* **91**, 357 (1993).
- [13] H. Z. Cummins, W. M. Du, M. Fuchs, W. Götze, A. Latz, G. Li, and N. J. Tao, *Physica A* **201**, 207 (1993).
- [14] W. Steffen, A. Patkowski, H. Gläser, G. Meier, and E. W. Fischer, *Phys. Rev. E* **49**, 2992 (1994).
- [15] W. Petry, E. Bartsch, F. Fujara, M. Kiebel, H. Sillescu, and B. Farago, *Z. Phys. B* **83**, 175 (1991).
- [16] B. Frick, B. Farago, and D. Richter, *Phys. Rev. Lett.* **64**, 2921 (1990).
- [17] F. Fujara, B. Geil, H. Sillescu, and G. Fleischer, *Z. Phys. B* **88**, 195 (1992).
- [18] P. Taborek, R. N. Kleiman, and D. J. Bishop, *Phys. Rev. B* **34**, 1835 (1986).
- [19] E. Rössler, *Phys. Rev. Lett.* **65**, 1595 (1989).
- [20] P. K. Dixon and S. R. Nagel, *Phys. Rev. Lett.* **61**, 341 (1988).
- [21] N. O. Birge and S. R. Nagel, *Phys. Rev. Lett.* **54**, 2674 (1985); N. O. Birge, *Phys. Rev. B* **34**, 1631 (1986).
- [22] M. Settles, F. Post, D. Müller, A. Schulte, and W. Doster, *Biophys. Chem.* **43**, 107 (1992).
- [23] H. Leyser, Diploma thesis, TU München, 1994.
- [24] W. Götze and L. Sjögren, *J. Phys. C* **20**, 879 (1987).
- [25] C. P. Lindsey and G. D. Patterson, *J. Chem. Phys.* **73**, 3348 (1980).
- [26] M. Naoki, H. Endou, and K. Matsumoto, *J. Phys. Chem.* **91**, 4169 (1987).
- [27] G. Fytas, T. Dorfmueller, and C. H. Wang, *J. Chem. Phys.* **87** 5041 (1983).
- [28] E. McLaughlin and A. R. Ubbelohde, *Trans. Faraday Soc.* **54**, 1804 (1958); R. J. Greet and D. Turnbull, *J. Chem. Phys.* **46**, 1243 (1967); W. T. Laughlin and D. R. Uhlmann, *J. Phys. Chem.* **76**, 2317 (1972); M. Cuckierman, J. W. Laue, and D. R. Uhlmann, *J. Chem. Phys.* **59**, 3639 (1973).
- [29] E. W. Fischer, *Physica A* **201**, 183 (1993).
- [30] T. N. Andrews and A. R. Ubbelohde, *Proc. R. Soc. London Ser. A* **228**, 435 (1955).
- [31] M. Naoki and S. Koeda, *J. Phys. Chem.* **93**, 948 (1989).